THE JOURNAL OF BIOLOGICAL CHEMISTRY Vol. 273, No. 10, Issue of March 6, pp. 5851–5857, 1998
Printed in U.S.A.

Genomic Organization, Chromosomal Localization, Tissue Distribution, and Biophysical Characterization of a Novel Mammalian *Shaker*-related Voltage-gated Potassium Channel, Kv1.7*

(Received for publication, September 8, 1997, and in revised form, December 16, 1997)

Katalin Kalman, Angela Nguyen, Julie Tseng-Crank‡§, Iain D. Dukes‡, Grischa Chandy, Carolyn M. Hustad¶, Neal G. Copeland¶, Nancy A. Jenkins¶, Harvey Mohrenweiser‖, Brigitte Brandriff‖, Michael Cahalan, George A. Gutman, and K. George Chandy‡‡**

*From the Departments of Physiology and Biophysics, and **Microbiology and Molecular Genetics, University of California Irvine, Irvine, California 92697; ‡Glaxo-Wellcome Research Institute, Research Triangle Park, North Carolina 27709; ¶Mammalian Genetics Laboratory, ABL-Basic Research Program, NCI-Frederick Cancer Research and Development Center, Frederick, Maryland 21702; and ‖Human Genome Center, Lawrence Livermore National Laboratory, Livermore, California 94550*

We report the isolation of a novel mouse voltage-gated *Shaker*-related K^+ channel gene, *Kv1.7* (*Kcna7*/*KCNA7*). Unlike other known Kv1 family genes that have intronless coding regions, the protein-coding region of *Kv1.7* is interrupted by a 1.9-kilobase pair intron. The *Kv1.7* gene and the related *Kv3.3* (*Kcnc3*/*KCNC3*) gene map to mouse chromosome 7 and human chromosome 19q13.3, a region that has been suggested to contain a diabetic susceptibility locus. The mouse Kv1.7 channel is voltage-dependent and rapidly inactivating, exhibits cumulative inactivation, and has a single channel conductance of 21 pS. It is potently blocked by noxiustoxin and stichodactylatoxin, and is insensitive to tetraethylammonium, kaliotoxin, and charybdotoxin. Northern blot analysis reveals ~3-kilobase pair *Kv1.7* transcripts in mouse heart and skeletal muscle. *In situ* hybridization demonstrates the presence of *Kv1.7* in mouse pancreatic islet cells. *Kv1.7* was also isolated from mouse brain and hamster insulinoma cells by polymerase chain reaction.

Ion channels that exhibit a variety of gating patterns and ion selectivity are critical elements that transduce signals in diverse cell types (1). Voltage-gated potassium-selective (Kv)[1] channels represent the largest family within this class of proteins (2), and perform many vital functions in both electrically excitable and nonexcitable cells. Following initiation of an action potential in nerve and muscle cells, Kv channels play the important role of repolarizing the cell membrane (1). Kv channels can also modulate hormone secretion, for example insulin release from pancreatic islet cells (3–6), and regulate calcium signaling during mitogen-stimulated activation of lymphocytes (7).

Kv channels in mammalian cells are encoded by an extended family of at least nineteen genes (2). The largest subfamily, *Kv1*, is related to the fly *Shaker* gene and contains six members, *Kv1.1–Kv1.6* (2). The *Shaker* gene has 21 exons, which can be alternatively spliced to generate at least five functionally distinct transcripts (8, 9). In contrast, the protein-coding regions of each of the six known mammalian *Kv1* genes and the three known *Xenopus* homologues are contained in a single exon (2, 10), precluding alternative splicing as a means of generating functionally different proteins. The evolutionary significance of this pattern of organization remains a puzzle.

Here we report the identification of a novel mammalian gene, *Kv1.7* (*Kcna7*/*KCNA7*), that has a genomic organization distinct from the other members of the vertebrate *Kv1* subfamily. We have defined the chromosomal location of this gene in the mouse and human genome, determined its tissue distribution, and characterized the biophysical and pharmacological properties of the cloned channel.

EXPERIMENTAL PROCEDURES

Isolation and Characterization of mKv1.7, hKv1.7, hKv3.3, and hKv3.4 DNA Clones—Three overlapping genomic clones (KC225, KC254, and KC256) were isolated from an AKR/J mouse genomic library screened with a mixture of *mKv1.1* and *rKv1.5* cDNA probes, as described previously (10), and mapped by multiple and partial restriction endonuclease digests, and by dideoxy sequencing. *Kv1.7* cDNAs were amplified by the polymerase chain reaction (PCR) from mouse brain and from the hamster insulinoma cell line, HIT-T1S, using intron-flanking primers (5′-TCTCCGTACTCGTCATCCTGG-3′ within S1 and 5′-AAATGGGTGTCCACCCGGTC-3′ on the 3′ side of S5). The resulting 588-bp PCR fragments were sequenced.

Cosmid clones encoding *hKv1.7* and *hKv3.3* (11) were isolated from a human chromosome 19-enriched library, Library F (12), screened with *mKv1.7* and *mKv3.3* probes. A 1.9-kb cDNA fragment of the *Shaw* family gene, *hKv3.4*, was isolated from a human pancreatic library (13) screened with a mixture of *hKv3.1* (0.9-kb *Xba*I/*Hin*dIII), *hKv3.3* (1.4-kb *Pst*I/*Eco*RI), and *mKv3.4* (0.9-kb *Hin*dII/*Eco*RI) probes at a final stringency of 0.5 × SSC and 0.1% SDS at 55 °C (8×10^6 phage screened). The isolated clone spans the region from S1 through the 3′ end of the coding region (0.6 kb), and 1.3 kb of the 3′-noncoding region.

Mice—Pancreatic tissue sections were obtained from 9–16-week-old diabetic-prone (*db*/*db*) and healthy (*db*/+) C57BL/KsJ mice. Mice ho-

* This work was supported in part by United States Public Health Service Grants AI-24783, Shannon Award GMOD54872 (to K. G. C.), and NS14609 (to M. D. C.); by Glaxo Inc. (to K. G. C.); by United States Department of Energy Contract W-7405-Eng-48 (to H. W. and B. B.); and by the National Institutes of Health, NCI, DHHD, under Contract NO1-CO-74101 with ABL (C. M. H., N. G. C., and N. A. J.). The costs of publication of this article were defrayed in part by the payment of page charges. This article must therefore be hereby marked "*advertisement*" in accordance with 18 U.S.C. Section 1734 solely to indicate this fact.

The nucleotide sequence(s) reported in this paper has been submitted to the GenBank™/EBI Data Bank with accession number(s) AF032099–AF032101.

§ Present address: Wyeth Ayerst Research, Cardiovascular/Metabolic Disease, CN8000, Rm. 1119A, Princeton, NJ 08543.

‡‡ To whom correspondence should be addressed: Rm. 291, Joan Irvine Simth Hall, Department of Physiology and Biophysics, Medical School, University of California Irvine, Irvine, CA 92697. Tel.: 714-824-2133; Fax: 714-824-3143; E-mail: gchandy@uci.edu.

[1] The abbreviations use are: Kv, voltage-gated potassium selective; PCR, polymerase chain reaction; RBL, rat basophilic leukemic; bp, base pair(s); mb, millibase pair(s); kb, kilobase pair(s).

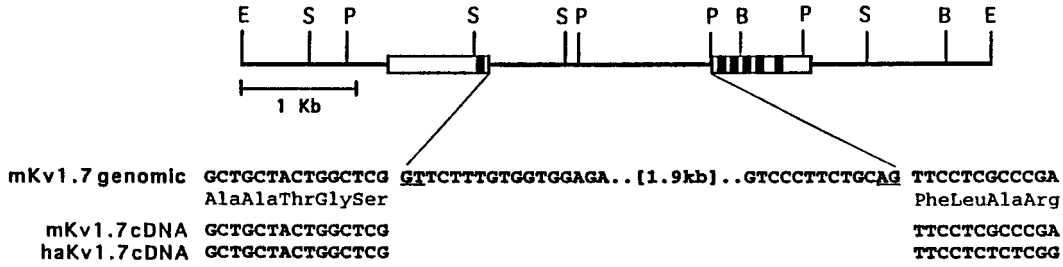

FIG. 1. **Genomic organization of mouse *Kv1.7*.** *Top*, the *mKv1.7* coding sequence is indicated by the two *stippled boxes*, and the six *bars* within these regions indicate the putative membrane-spanning domains S1 through S6. Restriction sites are indicated as follows: *B*, *Bgl*II; *E*, *Eco*RI; *P*, *Pst*I; *S*, *Sac*I. *Bottom*, comparison of the genomic sequence of *mKv1.7* with that of mouse and hamster (*haKv1.7*) cDNAs shows the splice donor and acceptor sites which form the boundaries of the single intervening sequence.

mozygous for the autosomal recessive diabetic susceptibility gene *db*, a mutated form of the leptin receptor (14, 15) on chromosome 4, develop diabetes beginning at about 6 weeks of age (16).

Mapping Mouse and Human Chromosomal Locations of Kv1.7 and Kv3.3—Interspecific backcross progeny were generated by mating (C57BL/6J × *Mus spretus*)F_1 females and (C57BL/6J) males, and a total of 205 N_2 mice were used to map the two mouse genes, *mKv1.7*/*Kcna7* and *mKv3.3*/*Kcnc3*, as described previously (11, 17–20). The probe for *mKv1.7* was the entire 6.4-kb *Eco*RI fragment shown in Fig. 1, and that for mouse *Kv3.3* was a 4-kb genomic *Hin*dIII fragment containing the entire 3′-exon (11). Although 155 mice were analyzed for all markers and are shown in this segregation analysis, up to 188 mice were typed for some pairs of markers. Recombination frequencies were calculated as described (11, 17–20) using the computer program SPRETUS MADNESS. Gene order was determined by minimizing the number of recombination events required to account for the allele distribution patterns. Fluorescent *in situ* hybridization of cosmids to metaphase human chromosomes was carried out as described previously (21, 22).

Northern Blot Assays—A Northern blot of poly(A)$^+$ RNA from mouse heart, brain, spleen, lung, liver, skeletal muscle, kidney, and testis (CLONTECH Inc., Palo Alto, CA) was probed with the mouse *Kv1.7*-specific 3′-noncoding region sequence. The *Pst*I/*Sac*I *Kv1.7* 3′-noncoding region was labeled by the random primer method (Boehringer Mannheim Random Primed DNA labeling kit). The RNA blot was hybridized at 60 °C for 18 h, washed at a final stringency of 0.2 × SSC and 0.1% SDS at 60 °C for 1 h, and exposed to x-ray film at −80 °C with an intensifying screen for 3 days.

In Situ Hybridization—cRNA probes labeled with α-^{35}S-labeled UTP (1300 Ci/mmol) were alkaline-denatured to an average size of 100 nucleotides and used for *in situ* hybridization on pancreatic frozen sections (6–10 μm thick) from *db*/*db* mice. Briefly, sections were hybridized overnight at 42 °C, RNase treated, washed five times in 0.5 × SSC at 65 °C, coated with Ilford K5 photographic emulsion, and exposed at 4 °C for varying times. After development, the sections were counterstained with hematoxylin and eosin Y and examined with a Leitz Aristoplan microscope equipped with reflected polarized light to visualize silver grains in dark field. The probes used for hybridization were as follows: *insulin*, 1.6-kb human insulin gene including the 5′- and 3′-flanking sequences (ATCC no. 57399); *hKv3.4*, 1.9-kb cDNA fragment spanning S1 through the 3′ end of the coding region (0.6 kb), and 1.3 kb of the 3′-noncoding region; *mKv1.7*, 540-bp *Pst*I/*Sac*I fragment containing 29 bp of C-terminal coding sequence and 511 bp of 3′-noncoding sequence.

Electrophysiological Studies—To make a *mKv1.7* expression construct we amplified a 588-bp fragment from mouse brain cDNA spanning the region encoded by the two Kv1.7 exons using reverse transcriptase PCR (5′-primer, 5′-TCTCCGTACTCGTCATCCTGG-3′; 3′-primer, 5′-AAATGGGTGTCCACCCGGTC-3′). Exon 1 (850-bp *Bsp*HI/*Bin*I fragment), a 283-bp *Bin*I/*Bgl*II fragment of our 588-bp PCR product, and exon 2 (747-bp *Bgl*II/*Hin*dIII), were ligated together at *Bin*I and *Bgl*II sites to generate "fragment I" (1880 bp). Fragment I was blunt-ended at the 5′ end and cloned into the pBluescript vector at *Sma*I/*Hin*dIII sites. To remove the 5′-NCR from fragment I, and for the purpose of cloning this fragment into the pBSTA expression vector, we introduced a unique *Bam*HI site just upstream of the initiator methionine using PCR: 5′-primer, 5′-ACAAAAGCTTCATATGACTACAAGGAAAGCT-3′; and 3′-primer: 5′-AAGCGCAACCCGGCCACG-3′. The resulting PCR product (corresponding to the first 233 nucleotides of the coding region) was spliced to fragment I at the *Nco*I site, and the 1870-nucleotide fragment was ligated to the pBSTA vector.

mKv1.7 cRNA was transcribed *in vitro* (Ambion Kit, Austin, TX) and diluted in a 0.1–0.5% fluorescein-dextran (M_r 10,000, Molecular Probes, Eugene, OR) in 100 mM KCl. Rat basophilic leukemic (RBL) cells were maintained in Dulbecco's modified Eagle's medium supplemented with 10% fetal calf serum (Hyclone, Logan, UT) and glutamine, and were plated onto glass coverslips one day prior to use for electrophysiological experiments. RBL cells were injected with cRNA using pre-pulled injection capillaries (Femtotip) in combination with an Eppendorf microinjection system (micromanipulator 5171 and transjector 5242; Madison, WI) as described previously (23). Four to six hours later, fluorescent cRNA-injected cells were evaluated electrophysiologically.

All membrane currents were recorded at room temperature (22–26 °C) with a LIST EPC-7 amplifier (Heka Elektronik, Germany). Series resistance compensation was employed if the current exceeded 2 nA, and the command input was controlled by a PDP 11/73 computer via a digital-to-analog converter. Capacitative and leak currents were subtracted using a P/8 procedure and the holding potential in all experiments was −80 mV. When membrane currents exceeded 2 nA 80% series resistance compensation was used.

RESULTS

The Protein-coding Region of mKv1.7 Contains an Intron Unlike Its Vertebrate Homologues

A restriction map of a 6.4-kb *Eco*RI DNA fragment containing the entire mouse *Kv1.7* coding region is shown in Fig. 1. The coding region is contained in two exons separated by a 1.9-kb intron. The upstream exon encodes the entire N terminus, S1, and part of the S1-S2 loop. The downstream exon contains the region extending from the S1-S2 loop to the C-terminal end of the protein. The intron-exon splice sites were determined by comparing the genomic sequence with cDNA sequences obtained from the hamster insulinoma cell line, HIT-T1S, and from mouse brain (Fig. 1).

The complete coding sequence of the *mKv1.7* is shown in Fig. 2. The mKv1.7 sequence is identical in the N terminus from bp 52 to 996 with the mouse EST sequence AA021711. Betsholtz *et al*. (24) amplified a short segment of Kv1.7 cDNA spanning the S5/S6 region from mouse (MK-6), rat (RK-6), and hamster (HaK-6) insulin-producing cells using PCR. Our sequence is identical to their MK-6 sequence, except for four nucleotide changes.

The deduced mKv1.7 protein consists of 532 amino acids and contains six putative membrane-spanning domains, S1–S6 (Fig. 2). The hydrophobic core of this protein shares considerable sequence similarity with other *Shaker* family channels, while the intracellular N and C termini and the external loops between S1/S2 and S3/S4 show little conservation. The protein contains conserved sites for post-translational modifications as indicated in Fig. 2. As do all other *Shaker*-related channels, mKv1.7 has a potential tyrosine kinase phosphorylation site (RPSFDAVLY) in its N-terminal region (2); the proline-rich stretch within the N terminus (see residues 29–42) may be a binding site for SH3 domains of tyrosine kinases. Two protein kinase C consensus sites (Ser/Thr-*X*-Arg/Lys) are present in the cytoplasmic loop between S4 and S5 of mKv1.7; at least one

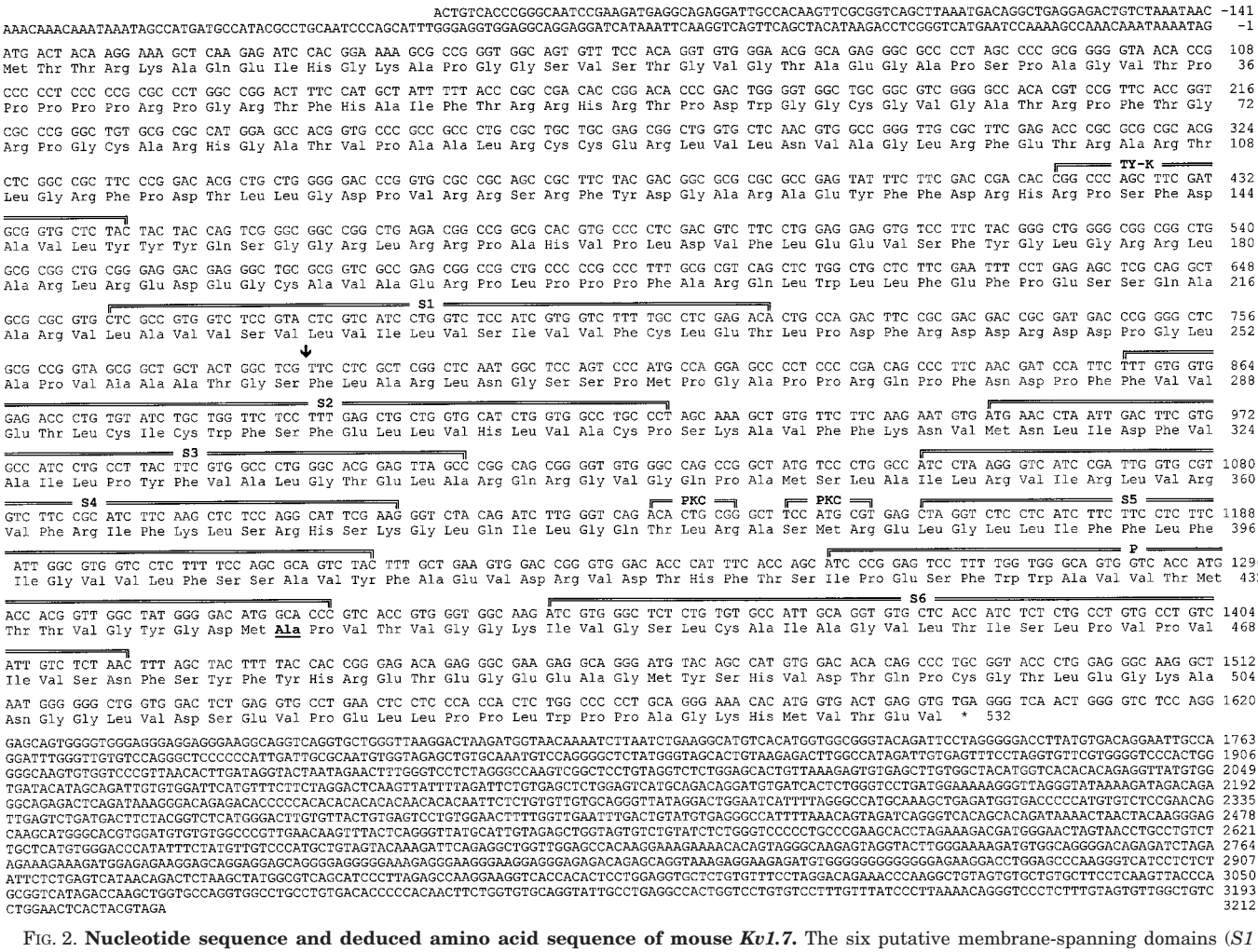

FIG. 2. **Nucleotide sequence and deduced amino acid sequence of mouse *Kv1.7*.** The six putative membrane-spanning domains (*S1* through *S6*) and pore-forming region (*P*) are indicated. The potential sites for phosphorylation by tyrosine kinase (*TY-K*) and protein kinase C (*PKC*) are shown. The position of the single intron between S1 and S2 is indicated by an *arrow*, and the critical residue for tetraethylammonium block (Ala-441, within the P region) is shown in *bold* and *underlined*.

of these sites is present in all members of the Kv1 family (2). mKv1.7, like Kv1.6, lacks an *N*-glycosylation site in the extracellular loop linking the S1 and S2 transmembrane segments; this consensus sequence is conserved in all other Kv1 family genes.

Fig. 3 shows a phylogenetic tree of the entire *Shaker* family of genes based on parsimony analysis of a nucleotide sequence alignment (generated from the amino acid sequence alignment) using the program PAUP (25). Our analysis places *mKv1.7* within the *Shaker* family of genes. The *mKv1.7* gene does not cluster with any of the known genes, and its position within the tree is not firmly established.

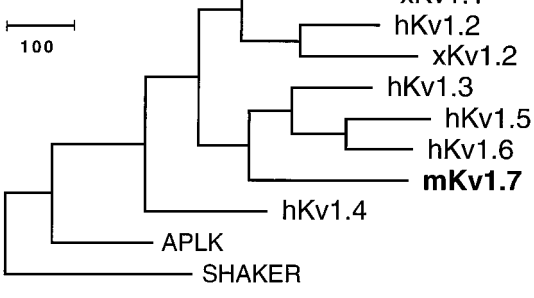

FIG. 3. **Proposed phylogenetic relationship of *mKv1.7* and other *Shaker*-related *Kv* channel genes.** This tree is based on parsimony analysis of nucleotide sequence alignments using the program PAUP (25). Horizontal distance represents the number of nucleotide substitutions in each lineage, with the *scale bar* at the *upper left* representing 100 substitutions. *m*, mouse; *h*, human; *x*, *Xenopus*; *APLK*, *Aplysia*; *SHAKER*, *Drosophila Shaker*.

Kv1.7 Is Located on Mouse Chromosome 7 and Human Chromosome 19q13.3

The *mKv1.7*/*Kcna7* gene resides on mouse chromosome 7 (Fig. 4*A*), ~0.5 centimorgan telomeric to the *Shaw*-related K^+ channel gene, *mKv3.3*/*Kcnc3*, and ~2.4 centimorgans centromeric of *MyoD1* (myoblast differentiation factor). The most centromeric marker in this study was *Gpi1* (glucose phosphate isomerase 1), which mapped ~6.1 centimorgans centromeric to *mKv3.3*/*Kcnc3*.

The interval on mouse chromosome 7 containing *mKv1.7*/*Kcna7* and *mKv3.3*/*Kcnc3* shares a region of homology with human chromosomes 19q13 and 11p15, and the human homologues of these K^+ channel genes may therefore be expected to reside on one of these chromosomes. Confirming this prediction, we mapped both genes to human 19q13.3–13.4 using fluorescent *in situ* hybridization. The idiogram of human chromosome 19 shown in Fig. 4*B*, and a more detailed map shown in Fig. 4*C*, indicate that *hKv1.7*/*KCNA7* is located ~1.3 mb centromeric of *hKv3.3*/*KCNC3*. The genes for both muscle glycogen synthase (*GYS1*) and the histidine-rich calcium protein (*HRC*) also map to this region; Kv1.7/KCNA7 lies ~25 kb telomeric to GYS1 and ~200 kb centromeric to HRC (Fig. 4*C*).

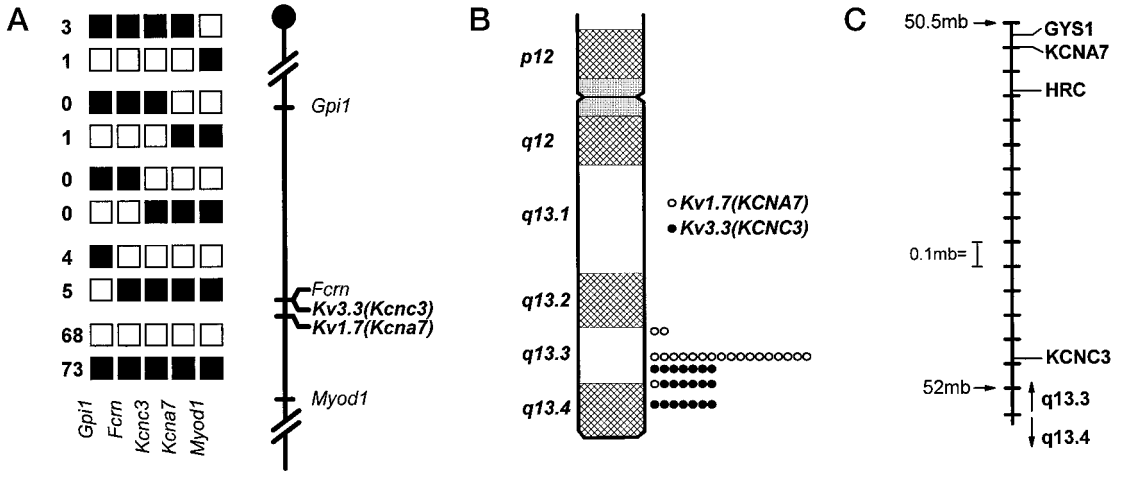

FIG. 4. **Chromosomal localization of the mouse and human *Kv1.7* genes.** *A*, mouse chromosome 7. (*Left*) results of segregation analysis in a (C57BL/6J × *M. spretus*)F_1 × C57BL/6J interspecific backcross. The genes indicated are as follows: *Gpi1*, glucose phosphate isomerase-1; *Fcrn*, Fc-receptor, neonatal form; *Myod1*, myoblast differentiation factor-1. The ratios of the total number of mice exhibiting recombinant chromosomes to the total number of mice analyzed for each pair of loci are *Gpi1* - 11/181 - *Fcrn* - 0/184 - *mKv3.3/Kcnc3* - 1/188 - *mKv1.7/Kcna7* - 4/167 - *Myod1*. The recombination frequencies expressed as genetic distances in centimorgans ± the S.E are: *Gpi1* - 6.1 ± 1.8 - [*Fcrn*, *mKv3.3*] - 0.5 ± 0.5 - *mKv1.7* - 2.4 ± 1.2 - *MyoD1*. *Filled boxes* indicate the presence of the C57Bl/6J allele, and *open boxes* the presence of the *M. spretus* allele. (*Right*) diagram showing the deduced order of *Kv1.7* and neighboring genes on mouse chromosome 7, with the centromere shown at the *top*. *B*, human chromosome 19. Diagram shows the deduced order of genes on human chromosome 19. A single *hKv1.7/KCNA7* cosmid was mapped to 19q13.3 by fluorescent *in situ* hybridization (FISH). Ten cells were scored for each cosmid used, and for each of two *hKv3.3/KCNC3* cosmids, signal was present on both chromatids in a position corresponding to 19q13.3-q13.4. The positions where signal was observed for the two probes are indicated as *open circles* (*hKv1.7/KCNA7*) and *solid circles* (*hKv3.3/KCNC3*). *C*, detailed map of the relevant region of human chromosome 19. The positions of *KCNA7*, *KCNC3*, *GYS1*, and *HRC* are shown, with each *cross-bar* indicating a distance of 100 kb. The positions corresponding to 50.5 and 52 mb of chromosome 19 (37) are indicated, as is the point of demarcation between chromosome bands q13.3 and q13.4.

Interestingly, a putative diabetes susceptibility gene has been suggested to be present at 19q13.3 (26, 27), especially in Finnish families with associated hypertension and difficulties in insulin-stimulated glucose storage. This region has also been suggested to contain a modifier locus for cystic fibrosis (28).

Biophysical and Pharmacological Characterization of Kv1.7 Channels

We carried out a detailed characterization of mKv1.7 channels expressed in RBL cells which express no native Kv currents (29, 30). The *mKv1.7* gene expressed in *Xenopus* oocytes produced currents (data not shown) similar to those obtained in RBL cells (Fig. 5).

Voltage Dependence—Patch clamp studies were performed in the whole-cell mode. Fig. 5*A* shows a family of outward currents elicited by a 200 ms depolarizing pulse from a holding potential of −80 mV in RBL cells injected with *mKv1.7* cRNA; no outward currents were detected in control cells (data not shown). The currents activate rapidly, and from the conductance-voltage curve shown in Fig. 5*B* we determined that the 1/2 activation potential ($V_{1/2}$) is −20 mV.

Inactivation and Deactivation—Inactivation of mKv1.7 channels was rapid following a 200 ms depolarizing pulse from −80 to 40 mV (Fig. 5*A*). The rate of inactivation, measured by fitting the data to a single exponential function, yielded a time constant (τ_h) of 14 ± 2.1 ms (S.E., $n = 7$). As shown in Fig. 5*C*, the current became progressively smaller following repeated depolarizing pulses at 1-s intervals. This phenomenon, termed "cumulative inactivation," is due to the accumulation of channels in the inactivated state which are then unavailable for opening. The related channels, Kv1.3 (7) and Kv1.4 (31), also display this behavior.

The kinetics of channel closing (deactivation) was determined by first opening the channels with a 15 ms conditioning depolarizing pulse, and then forcing the channels to close by repolarizing to different potentials (Fig. 5*D*). The time constant, τ_{tail}, of the resulting "tail" current was 5.1 and 5.3 ms at −60 mV in two cells.

Single-channel Conductance—We measured single-channel currents in an outside-out patch by applying 450-ms voltage ramps from −90 to 80 mV every second (Fig. 5*E*). Single channel events were seen at potentials more positive than ~−15 mV. The single-channel conductance of 21 pS was estimated from the slope of the current recorded during an opening (Fig. 5*E*).

Pharmacology—We determined the pharmacological sensitivity of the mKv1.7 channel using methods described previously (30, 32), IC_{50} values in each case being determined when block reached steady-state. The channel was blocked by several non-peptide small molecule antagonists, 4-aminopyridine (IC_{50} = 245 μM), capsaicin (25 μM), cromakalim (450 μM), tedisamil (18 μM), nifedipine (13 μM), diltiazem (65 μM), and resiniferatoxin (20 μM). Surprisingly, the dihydroquinoline compound, CP-339,818, that blocks rapidly inactivating Kv1 channels in the nanomolar range (30), had little effect on mKv1.7 (IC_{50} = 10 μM). The channel was insensitive to externally applied tetraethylammonium (C_{50} = 86 mM), probably because the residue at the tetraethylammonium-binding site, Ala-441 (Fig. 2), is hydrophobic.

The mKv1.7 channel is also potently blocked by a peptide (ShK toxin) obtained from sea anemone *Stichodactyla helianthus* (IC_{50} = 13 nM), and by the scorpion toxins, noxiustoxin (IC_{50} = 18 nM) and margatoxin (IC_{50} = 116 nM). The channel was resistant to charybdotoxin (IC_{50} >1000 nM) and kaliotoxin (IC_{50} >1000 nM).

Expression of mKv1.7 Transcripts in Different Tissues

Northern blot assays using a mKv1.7-specific probe revealed strongly hybridizing 3-kb bands in heart and skeletal muscle; faint bands of similar size were visible in liver and lung (together with larger 7–8-kb bands), but none were seen in spleen, kidney, testis, or brain (Fig. 6) We were able to isolate *mKv1.7* transcripts from mouse brain by PCR (see Fig. 1). mKv1.7 is also expressed in placenta, since the mouse EST AA021711 was derived from this tissue.

PCR analysis demonstrated the presence of haKv1.7 mRNAs

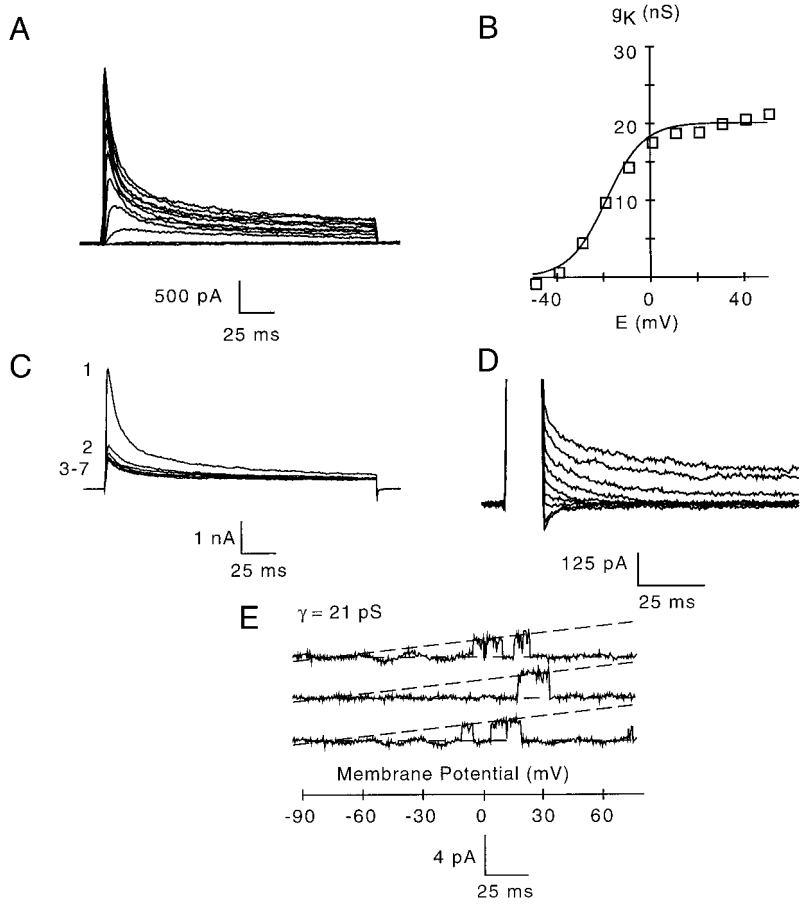

FIG. 5. **Kv1.7 currents.** *A*, family of mKv1.7 currents. The holding potential was −80 mV and depolarizing pulses were applied every 30 s. The test potential was changed from −50 to 50 mV in 10-mV increments. *B*, peak K^+ conductance-voltage relation for currents shown in *A*. The line through the points was fitted with the Boltzmann equation: $g_k(E) = g_{k(\max)}/\{1 + \exp[(E_n - E)/k]\}$, with parameter values $g_{k(\max)}$ = 20 nS and k = −8 mV. *C*, cumulative inactivation of Kv1.7 currents. Currents were elicited by a train of six depolarizing voltage steps (200-ms duration) to 40 mV once every second from a holding potential of −80 mV. The current amplitude decreases significantly during this train of pulses from the largest (*first trace*) to the smallest (*last*). *D*, kinetics of deactivation of Kv1.7 currents. Tail currents were elicited by voltage steps from −100 to −40 mV after a 15-ms depolarizing prepulse to 40 mV. The tail current-decay time constants, τ_t, were measured by fitting single-exponential functions to the decay of the K^+ current during repolarization. *E*, single-channel currents of Kv1.7 in an outside-out patch. The *broken line* shows the slope conductance.

in hamster insulinoma cells (Fig. 1). We verified the presence of *mKv1.7* mRNA in pancreatic islet cells obtained from 9–16-week-old diabetic *db/db* mice by *in situ* hybridization (Fig. 7*C*) using a mKv1.7-specific antisense probe (12–14); *mKv1.7* mRNA was also present in islets from normal *db/+* mice (data not shown). Scattered acinar cells outside the islets also showed mKv1.7 hybridization (Fig. 7*C*). In contrast, *mKv3.4* mRNA was found in acinar cells surrounding islets, but not in islets, of both *db/db* (Fig. 7B) and *db/+* mice (data not shown). As a control, insulin mRNA was detected in both normal and diabetic islets, but not in acinar cells (Fig. 7*A*). A *Kv1.5*-specific probe did not show appreciable hybridization to islets (data not shown), despite a report of *Kv1.5* cDNA having been cloned from human insulinoma cells (33).

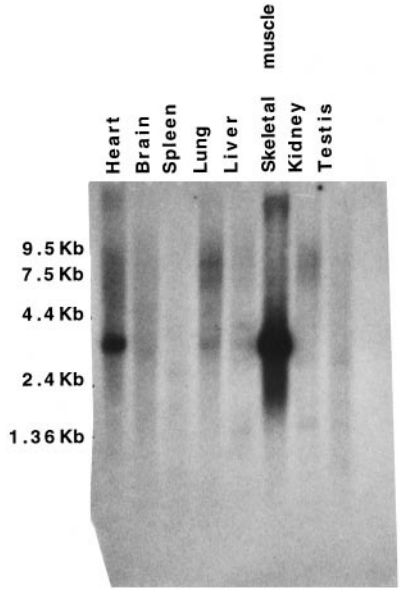

FIG. 6. **Expression of *Kv1.7* mRNA in tissues.** Northern blot assay.

DISCUSSION

Unlike all other known mammalian *Shaker*-related genes (*Kv1.1–Kv1.6*) that have intronless coding regions (2, 9), the protein-coding region of *mKv1.7* is interrupted by a single 1.9-kb intron. The fly *Shaker* gene also contains an intron in the S1-S2 loop, raising the possibility that the intron in *Kv1.7* may be ancient, predating the divergence of flies and mammals. Both the mouse *Kv.1.7* and the fly *Shaker* intron are placed between codons, *i.e.* they are "phase 0" introns. While this is consistent with their having a common origin it may also be fortuitous, since there are only three possible "phases." Although we favor the idea that Kv introns were lost in the vertebrate lineage before their expansion by gene duplication (in which case the *Kv1.7* intron would represent a more recent insertion), the evolutionary history of this complex gene family remains to be elucidated.

Since *Kv1.7* mRNA is expressed in the mouse heart, we searched the literature for native cardiac A-type Kv currents with properties resembling those of Kv1.7. The Kv1.7 homotetramer shares many properties with the rapidly inactivating transient outward (I_{to}) current in cardiac Purkinje fibers, but not the I_{to} current in atrial and ventricular myocytes. Kv1.7 and the Purkinje I_{to} currents activate at negative potentials (∼−30 to −20 mV), inactivate rapidly (τ_h < 25 ms), exhibit cumulative inactivation, are blocked by micromolar concentrations of 4-aminopyridine, and are resistant to >20 mM tetra-

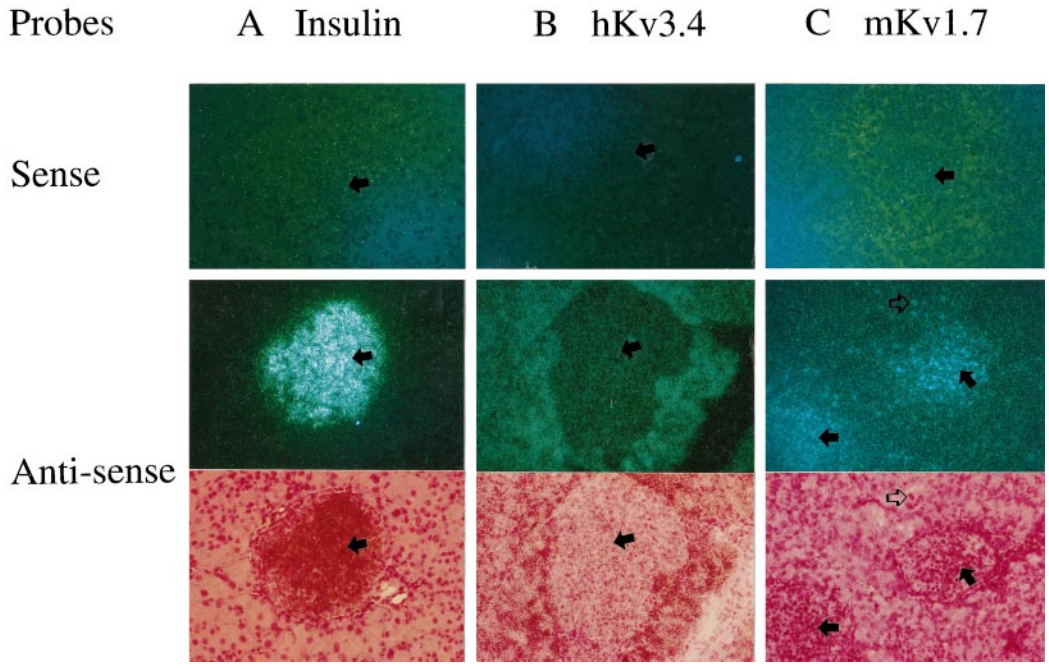

FIG. 7. ***In situ* hybridization of mouse pancreas from diabetic *db/db* mice showing expression of *Kv1.7*, *Kv3.4*, and *insulin*.** *A–C*, pancreatic sections from a *db/db* mouse hybridized with probes specific for insulin (*A*), Kv3.4 (*B*), or Kv1.7 (*C*). *Top*, sense probe, dark field; *middle*, antisense probe, dark field; *bottom*, antisense probe, bright field, showing the same field as the middle row. *Filled arrow*, pancreatic islet; *open arrow*, acinar cells that hybridized with *Kv1.7* antisense probe. *A*, sense and antisense probes, 0.1 ng/ml, 10 days of exposure; *B*, sense probe, 0.1 ng/μl, 10 days of exposure, and antisense probe, 0.5 ng/μl, 7 days of exposure; *C*, sense and antisense probes, 0.5 ng/μl, 1 month of exposure. Magnification: *A* and *B*, $\times$ 425; *C*, $\times$ 312.

ethylammonium (34–36) (this study). In contrast, the I_{to} current in atrial and ventricular muscle, a product of the *Kv4.3* gene, does not exhibit cumulative inactivation (36). These studies suggest that at least part of the Purkinje fiber I_{to} might be encoded by the *Kv1.7* gene, although more extensive biophysical and pharmacological studies are required to confirm the link, and the presence of *Kv1.7* mRNA and/or protein has yet to be demonstrated in these fibers. The abundant expression of *Kv1.7* mRNA in mouse heart suggests that this channel is also likely to be present in ventricular and/or atrial muscle where it may co-assemble with other Kv1 family channels to form heterotetramers.

Recent studies suggest an important role for Kv channels in regulating islet cell function, specifically in repolarizing the membrane potential following each action potential during the glucose-induced bursting phase associated with insulin secretion (3–6). Despite these interesting findings, the genes encoding *Kv* genes in β-cells have not been identified. Although the *Kv1.5* gene was isolated from human insulinoma cells (33), we did not detect *Kv1.5* mRNA in normal or diseased islets. We have, however, demonstrated the presence of *Kv1.7* mRNA in these cells. Unlike the noninactivating Kv channels in pancreatic β-cells (3, 4), the Kv1.7 homotetramer exhibits rapid C-type inactivation. Since *Kv1.7* mRNA is expressed in pancreatic islets, it is possible that heteromultimers composed of Kv1.7 and other Kv1 subunits constitute the native Kv channels in β-cells. Enhanced levels of such Kv channels would excessively hyperpolarize the membrane of β-cells and impair insulin secretion (5). The mapping of the *Kv1.7* gene to human chromosome 19q13.3, a region thought to contain a diabetic susceptibility gene (26, 27), also suggests that *Kv1.7* might contribute to the pathogenesis of type II diabetes mellitus in some humans.

In conclusion, we have described a novel *Kv1* family gene with a genomic organization distinct from all the other members of the family. The Kv1.7 channel produces a typical A-type current, and transcripts are expressed in the heart, skeletal muscle, brain, placenta, and pancreatic β-cells. This channel is biophysically and pharmacologically similar to the Purkinje fiber I_{to} current, and the gene may contribute at least one subunit to heteromultimeric Kv channels in pancreatic β-cells.

Acknowledgments—The assistance of F. Glaser, S. Plummer, B. Dethlefs, S. Hoffman, M. Christensen, T. Wymore, C. Chandy, and D. J. Gilbert is gratefully acknowledged. We are obliged to Dr. J. Aiyar for reading and improving our manuscript.

REFERENCES

1. Hille, B. (1993) *Ionic Channels of Excitable Membranes*, 2nd Ed., Sinauer, Sunderland, MA
2. Chandy, K. G., and Gutman, G. A. (1995) in *Handbook of Receptors and Channels: Ligand and Voltage-gated Ion Channels* (North, A., ed) pp. 1–72, CRC Press, Boca Raton, FL
3. Smith, P. A., Bokvist, K., Arkhammar, P., Berggren, P. O., and Rorsman, P. (1990) *J. Gen. Physiol.* **95,** 1041–1059
4. Smith, P. A., Ashcroft, F. M., and Rorsman, P. (1990) *FEBS Lett.* **261,** 187–190
5. Philipson, L. H., Rosenberg, M., Kuznetsov, A., Lancaster, M. E., Worley, J. F., III, Roe, M. W., and Dukes I. D. (1994) *J. Biol. Chem.* **269,** 27787–27790
6. Roe, M. W., Worley, J. F., 3rd, Mittal, A. A., Kuznetsov, A., DasGupta, S., Mertz, R. J., Witherspoon, S. M., 3rd, Blair, N., Lancaster, M. E., McIntyre, M. S., Shehee W. R., Dukes, I. D., and Philipson, L. H. (1996) *J. Biol. Chem.* **271,** 32241–32246
7. Lewis, R. S., and Cahalan, M. D. (1995) *Annu. Rev. Immunol.* **13,** 623–653
8. Pongs, O., Kecskemethy, N., Muller, R., Krah-Jentgens, I., Baumann, A., Kiltz, H. H., Canal, I., Llamazares, S., and Ferrsu, A. (1988) *EMBO J.* **7,** 1087–1096
9. Schwarz, T. L., Papazian, D. M., Caretto, R. C., Jan, Y. N., and Jan, L. Y. (1988) *Nature* **331,** 137–142
10. Chandy, K. G., Williams, C. B., Spencer, R. H., Aguilar, B. A., Ghanshani, S., Tempel, B. L., and Gutman, G. A. (1990) *Science* **247,** 973–975
11. Ghanshani, S., Pak, M., McPherson, J. D., Strong, M., Dethlefs, B., Wasmuth, J. J., Salkoff, L., Gutman, G. A., and Chandy, K. G. (1992) *Genomics* **12,** 190–196
12. deJong, P. J., Yokabata, K., Chen, C., Lohman, F., Pederson, L., McNinch, J., and van Dilla, M. (1990) *Cytogenet. Cell Genet.* **51,** 985
13. Permutt, M. A., Koranyi, L., Keller, K., Lacy, P. E., Scharp, D. W., and Mueckler, M. (1989) *Proc. Natl. Acad. Sci. U. S. A.* **86,** 8688–8692
14. Chen, H., Charlat, O., Tartaglia, L. A., Woolf, E. A., Weng, X., Ellis, S. J., Lakey, N. D., Culpepper, J., Moore, K. J., Breitbart, R. E., Duyk, G. M., Tepper, R., and Morgenstern, J. P. (1996) *Cell* **84,** 491–495
15. Lee, G. H., Proenca, R., Montez, J. M., Carroll, K. M., Darvishzadeh, J. G., Lee, J. I., and Friedman, J. M. (1996) *Nature* **379,** 632–635
16. Shafrir, E. (1992) *Diabetes Metab. Rev.* **8,** 179–208

17. Green, E. L. (1981) in *Genetics and Probability in Animal Breeding Experiments*, pp 77–113, Oxford University Press, New York
18. Jenkins, N. A., Copeland, N. G., Taylor, B. A., and Lee, B. K. (1982) *J. Virol.* **43,** 26–36
19. Saunders, A. M., and Seldin, M. F. (1990) *Genomics* **8,** 525–535
20. Copeland, N. G., and Jenkins, N. A. (1991) *Trends Genet.* **7,** 113–118
21. Brandriff, B. F., Gordon, L. A., Tynan, K. T., Olsen, A. S., Mohrenweiser, H. W., Fertitta, A., Carrano, A. V., and Trask, B. J. (1992) *Genomics* **12,** 773–779
22. Trask, B., Fertitta, A., Christensen, M., Youngblom, J., Bergmann, A., Copeland, A., de Jong, P., Mohrenweiser, H., Olsen, A., Carrano, A., and Tynan, K. (1993) *Genomics* **15,** 133–145
23. Ikeda, S. R., Soler, F., Zuhlke, R. D., Lewis, D. L. (1992) *Pflueg. Arch. Eur. J. Physiol.* **422,** 201–203
24. Betsholtz, C., Baumann, A., Kenna, S., Ashcroft, F. M., Ashcroft, S. J., Berggren, P. O., Grupe, A., Pongs, O., Rorsman, P., Sandblom, J., and Welsh, M. (1990) *FEBS Lett.* **263,** 121–126
25. Swofford, D. L. (1993) PAUP: Phylogenetic analysis using parsimony. Version 3.1. Computer program distributed by the Illinois Natural History Survey, Champaign, IL
26. Groop, L. C., Kankuri, M., Schalin-Jantti, C., Ekstrand, A., Nikula-Ijas, P., Widen, E., Kuismanen, E., Eriksson, J., Franssila-Kallunki, A., Saloranta, C., and Koskimies, S. (1993) *N. Engl. J. Med.* **328,** 10–14
27. Elbein, S. C., Hoffman, M., Ridinger, D., Otterud, B., and Leppert, M. (1994) *Diabetes* **43,** 1061–1065
28. Estivill, X. (1996) *Nat. Genet.* **12,** 348–350
29. McCloskey, M., and Cahalan, M. D. (1990) *J. Gen. Physiol.* **95,** 208–222
30. Nguyen, QA, Kath, J., Hanson, D. C., Biggers, M. S., Canniff, P. C., Donovan, C. B., Mather, R. J., Bruns, M. J., Rauer, H., Aiyar, J., Lepple-Wienhues, A., Gutman, G. A., Grissmer, S., Cahalan, M. D., and Chandy, K. G. *Mol. Pharmacol.* **50,** 1672–1679, 1996
31. Wymore, R., Korenberg, J. R., Coyne, C. Chen, X-N, Hustad, C., Copeland, N. G., Gutman, G. A., Jenkins, N. A., Chandy, K. G. (1994) *Genomics* **20,** 191–202
32. Grissmer, S., Nguyen, A. N., Aiyar, J., Hanson, D. C., Mather, R. J., Gutman, G. A., Karmilowicz, M. J., Auperin, D. D., and Chandy, K. G. (1994) *Mol. Pharmacol*. **45,** 1227–1234
33. Philipson, L. H., Hice, R. E., Schaefer, K., LaMendola, J., Bell, G. I., Nelson, D. J., and Steiner, D. F. (1991) *Proc. Natl. Acad. Sci. U. S. A.* **88,** 53–57
34. Reder, R. F., Miura, D. S., Danilo, P., Jr., and Rosen, M. R. (1981) *Circ. Res.* **48,** 658–668
35. Gintant, G. A., Cohen, I. S., Datyner, N. B., and Kline, R. P. (1992) in *The Heart and Cardiovascular System* (Fozzard, H., ed) 2nd Ed., pp. 1122–1166, Raven Press, New York
36. Dixon, J. E., Shi, W., Wang, H. S., McDonald, C., Yu, H., Wymore, R. S., Cohen, I. S., and McKinnon, D. (1996) *Circ. Res.* **79,** 659–668
37. Ashworth, L. K., Batzer, M. A., Brandriff, B., Branscomb, E., de Jong, P., Garcia, E., Garnes, J. A., Gordon, L. A., Lamerdin, J. E., Lennon G., Mohrenweiser, H., Olsen, A. S., Slezak, T., and Carrano, A. V. (1995) *Nat. Genet.* **11,** 422–427